Organic & Biomolecular Chemistry

www.rsc.org/obc

Volume 10 | Number 34 | 14 September 2012 | Pages 6805–7016

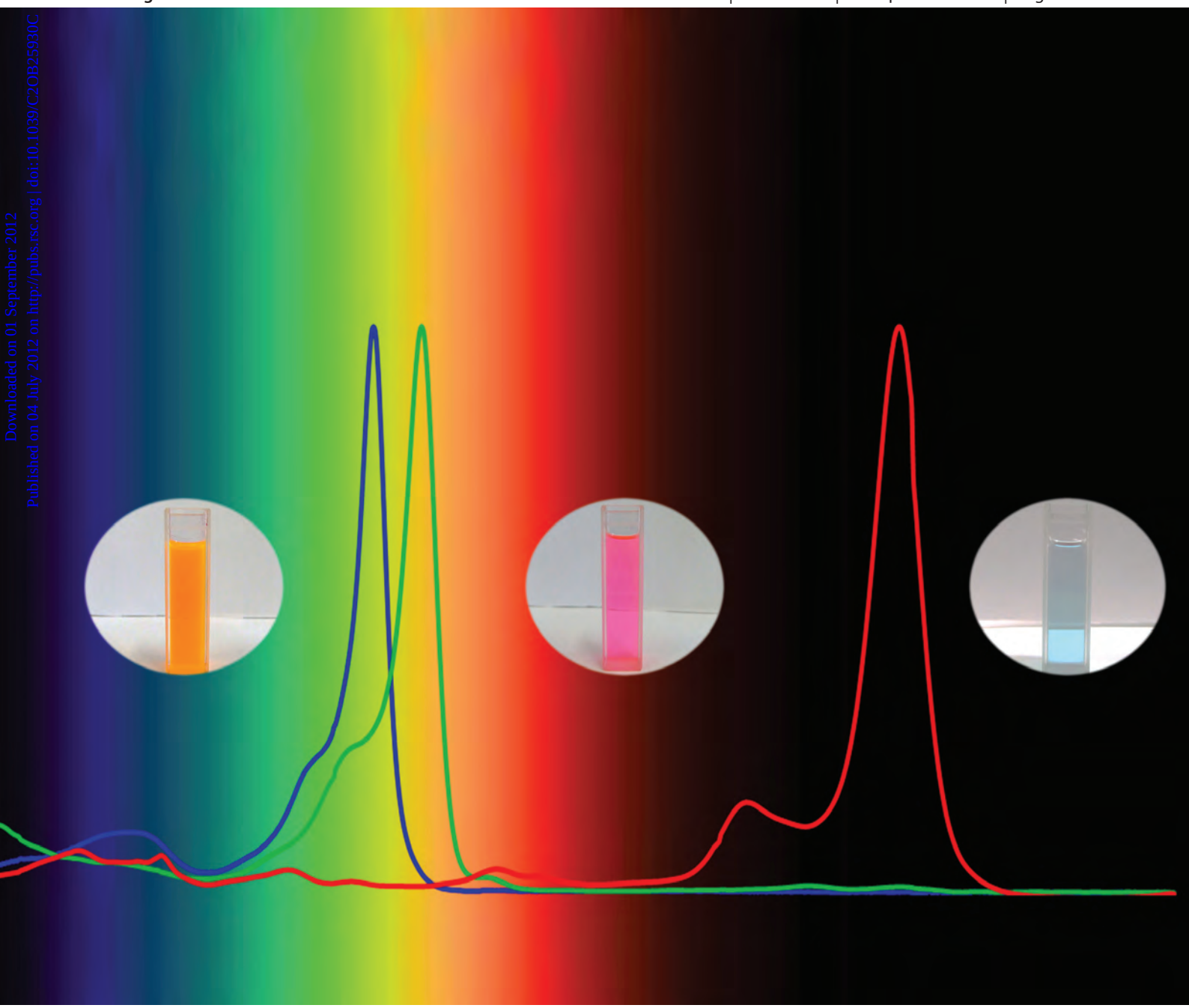

ISSN 1477-0520

RSC Publishing

FULL PAPER

Toshi Nagata, Hidemitsu Uno *et al.*

π-Fused bis-BODIPY as a candidate for NIR dyes

1477-0520(2012)10:34;1-A

Organic & Biomolecular Chemistry

Dynamic Article Links
View Online

Cite this: *Org. Biomol. Chem.*, 2012, **10**, 6840

www.rsc.org/obc

PAPER

π-Fused bis-BODIPY as a candidate for NIR dyes†

Mitsunori Nakamura,[a] Hiroyuki Tahara,[a] Kohtaro Takahashi,[a] Toshi Nagata,*[b] Hiroki Uoyama,[a] Daiki Kuzuhara,[d] Shigeki Mori,[c] Tetsuo Okujima,[a] Hiroko Yamada[d] and Hidemitsu Uno*[a]

Received 15th May 2012, Accepted 28th June 2012
DOI: 10.1039/c2ob25930c

Benzene-fused bis-(borondipyrromethene)s (bis-BODIPYs) were synthesized by retro-Diels–Alder reaction of the corresponding bicyclo[2.2.2]octadiene-fused (BCOD-fused) bis-BODIPYs, which were, in turn, prepared from 4,8-ethano-4,8-dihydropyrrolo[3,4-*f*]isoindole derivatives. The π-fused bis-BODIPY chromophores were designed to show intensive absorption and strong fluorescence in the near-infrared region and not to have any strong absorption in the visible region. A 6,10-dibora-5a,6a,9a,10a-tetraaza-*s*-indaceno[2,3-*b*:6,5-*b*′]difluorene derivative (*syn*-bis-benzoBODIPY) obtained by a thermal retro-Diels–Alder reaction of the corresponding BCOD-fused BODIPY dimer has strong absorption and emission bands at 775 and 781 nm, respectively. The absolute quantum yield is 0.36. The absorption is more than 5.0 times stronger than other absorptions observed in the visible region. In the case of 6,15-dibora-5a,6a,14a,15a-tetraaza-*s*-indaceno[2,3-*b*:6,7-*b*′]difluorene derivatives (*anti*-bis-benzoBODIPY), the absorption and emission maxima exceed 840 nm.

Introduction

Increasing interest has been paid towards chromophores with absorptions and emissions in the red or near-infrared (NIR) region. Organic compounds with such chromophores are thought to be promising materials for a broad range of applications in material science. Their applications such as photo-dynamic therapy dyes,[1] microscopic imaging agents,[2] semiconductors in NIR light emitting diodes,[3] dyes for NIR cut-filters,[4] and photo-sensitizers in NIR-utilizing solar cells[5] have been reported. In particular these materials are essential for the success of high performance organic solar cells.[6] The chromophores must consist of large conjugated π systems and are classified into two types: linear and cyclic chromophores. Generally, the latter chromophores show rather complicated absorption bands due to the existence of plural transitions between molecular orbitals with different symmetries near the HOMO and LUMO levels. These chromophores have rather large HOMO–LUMO gaps and are commonly robust in spite of abundant π electrons. This phenomenon is essential because cyclic chromophores have degenerated or nearly degenerated HOMOs and LUMOs due to the existence of a certain kind of symmetry. The porphyrin chromophore is a typical example; there are two major absorption bands, namely Soret and Q bands, in the UV-vis region mainly derived from transitions between HOMOs and LUMOs.[7] When these chromophores are fused, not only the absorption bands mainly due to the transitions between enlarged HOMOs and LUMOs but also other bands in the visible region due to monomeric transitions are usually observed.[8] On the other hand, linear chromophores show relatively simple absorptions. For example, boron-dipyrromethene (BODIPY)[9] and cyanine[10] dyes are well known to have simple strong absorption and emission bands in the visible region. When the BODIPY chromophore is fused with other chromophores in the *meso* direction, however, the absorption spectra become complicated due to the multi-directional transitions.[11] Recently, a German group successfully prepared selective NIR dyes. They used pyrrolopyrrole[12] as the cyanine-connecting unit and succeeded in the preparation of bis- and tris-cyanine dyes,[13] which had not only intense absorptions in the NIR region and good transparency in the visible region, but also very high fluorescence quantum yields.[13c] In this paper, we discuss our approach toward the preparation of selective NIR dyes by the fusion of BODIPY chromophores (Chart 1).

Results and discussion

We started the synthesis by preparation of BCOD-fused bis-pyrroles **2** from ethyl 4,7-dihydro-4,7-ethano-2*H*-isoindole-1-

[a]*Department of Chemistry and Biology, Graduate School of Science and Engineering, Ehime University, Matsuyama 790-8577, Japan. E-mail: uno@ehime-u.ac.jp; Fax: +81-89-927-9610*
[b]*National Institutes for Natural Sciences (NINS), Institute for Molecular Science (IMS), 5-1 Higashiyama, Myodaiji, Okazaki 444-8787, Japan*
[c]*Integrated Center for Sciences, Ehime University, Matsuyama 790-8577, Japan*
[d]*Graduate School of Materials Science, Nara Institute of Science and Technology, Ikoma 630-0192, Japan; CREST, JST, Chiyoda-ku, 102-0075, Japan*

†Electronic supplementary information (ESI) available: Other experimental data, X-ray data, and data indicated in the text. CCDC 865408, 864644–864652. For ESI and crystallographic data in CIF or other electronic format see DOI: 10.1039/c2ob25930c

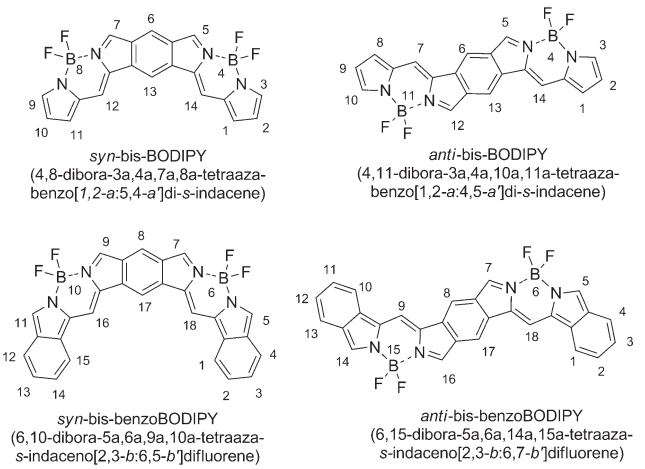

Chart 1 Skeletal nomenclature of bis-BODIPYs.

carboxylate (**1**)[14] according to the literature procedure.[8b] Addition of phenylsulfenyl chloride followed by oxidation with mCPBA and a modified Barton–Zard reaction[15] gave bis-pyrroles *syn*-**2** and *anti*-**2** as a diastereomeric mixture (4 : 3 ratio) in a total yield of 63%.[16] Chromatographic separation of the mixture afforded *syn*-**2** and *anti*-**2** in pure form (Scheme 1). Although reduction of bis-pyrroles *syn*-**2** and *anti*-**2** with $LiAlH_4$ in refluxing THF gives the corresponding dimethyl derivatives in good yields,[17] the dimethyl bis-pyrroles are rather labile toward acid and readily decompose under the acidic conditions employed in the preparation of dipyrromethanes. Therefore, the more stable di-esters *syn*-**2** and *anti*-**2** under acidic conditions were directly used for the dipyrromethane synthesis. Double dipyrromethane formation of *syn*-**2** and *anti*-**2** with ethyl 5-acetoxymethyl-3,4-diethylpyrrole-2-carboxylate (**3a**)[18] under acidic conditions (*p*-TsOH, AcOH) gave bis-dipyrromethane tetraesters *syn*-**4a** and *anti*-**4a** in 54% and 73% yields, respectively. Exhaustive reduction of *syn*-**4a** and *anti*-**4a** with $LiAlH_4$ in refluxing THF afforded tetramethyl derivatives *syn*-**5a** and *anti*-**5a** in respective yields of 96% and 93%. Oxidative complexation of the tetramethyl derivatives and $BF_3{\cdot}OEt_2$ with the aid of chloranil gave BCOD-connected bis-BODIPYs *syn*-**6a** and *anti*-**6a** in 36% and 53% yields, respectively. A similar synthesis using BCOD-fused acetoxymethylpyrrole **3b**[19] in the first bis-dipyrromethane formation was carried out to give *syn* and *anti* bis-BODIPYs *syn*-**6b** and *anti*-**6b** bearing three BCOD moieties, two of which were fused at the distal pyrrole rings. The overall yields of *syn*-**6b** and *anti*-**6b** were 28% and 48%, respectively.

The thermal behavior of the BCOD-fused bis-BODIPYs **6** was next examined by the thermogravimetric (TG) analysis. The measurements were conducted at a rate of 10 °C min^{-1} and the TG curves obtained are illustrated in Fig. 1. In all cases, theoretical weight is lost due to the extrusion of ethylene moieties except for a small quantity of solvent included in the samples. In the cases of *syn*- and *anti*-**6a**, the weight loss due to the retro-Diels–Alder reaction connecting the BODIPY chromophores started from 180 °C and ceased around 240 °C and no obvious weight decrease was observed below 300 °C. In the cases of *syn*- and *anti*-**6b**, there was an inflection point around 200 °C in the weight loss started around 150 °C. Double the amount of weight was lost in the lower temperature range before the inflection

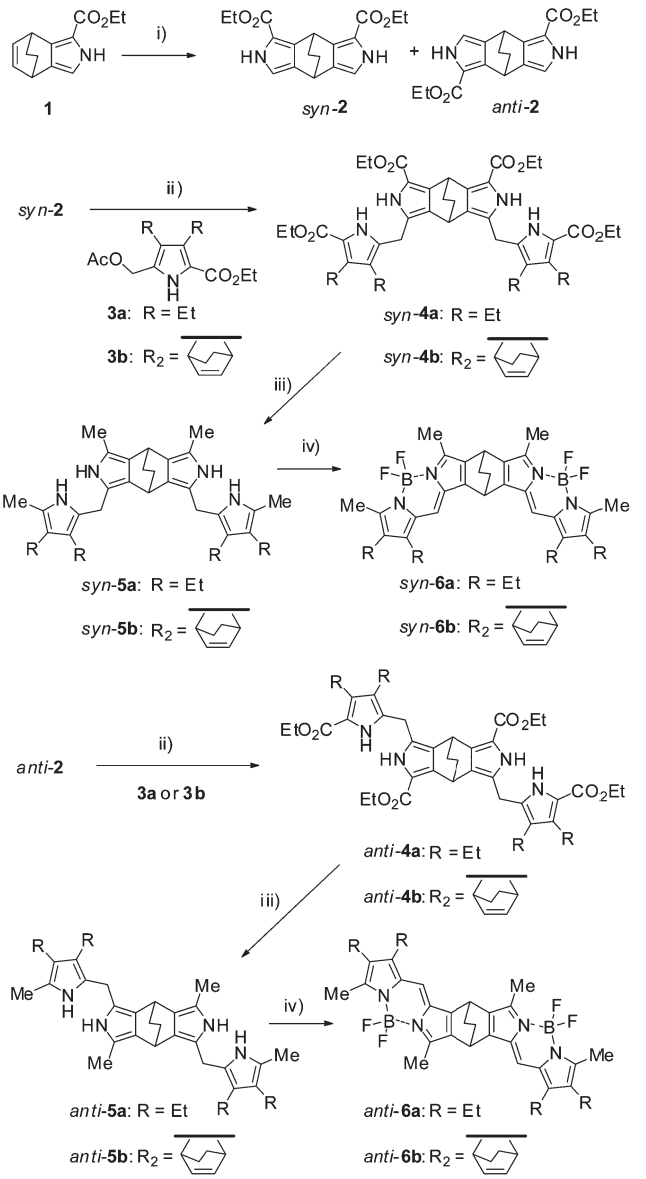

Scheme 1 *Reagents, conditions, and yields*: (i) ref. 11. (ii) **3**, *p*-TsOH, AcOH, rt; *syn*-**4a**, 54%; *syn*-**4b**, 61%; *anti*-**4a**, 73%; and *anti*-**4b**, 72%. (iii) $LiAlH_4$, THF, reflux; *syn*-**5a**, 96%; *syn*-**5b**, 65%; *anti*-**5a**, 93%; and *anti*-**5b**, 82%. (iv) chloranil, $BF_3{\cdot}OEt_2$, $(i\text{-}Pr)_2EtN$, CH_2Cl_2, rt; *syn*-**6a**, 36%; *syn*-**6b**, 70%; *anti*-**6a**, 53%; and *anti*-**6b**, 82%.

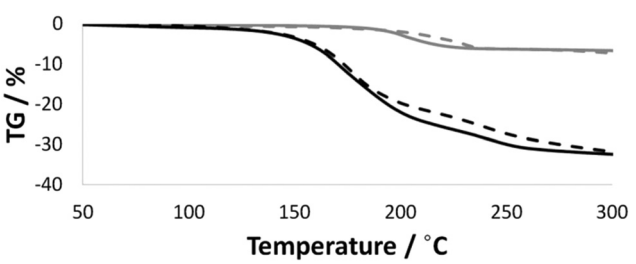

Fig. 1 TG curves (10 °C min^{-1}) of *syn*-**6a** (grey broken line), *anti*-**6a** (grey line), *syn*-**6b** (black broken line), and *anti*-**6b** (black line).

point and the higher temperature range corresponded to the temperature for the retro-Diels–Alder reaction connecting the BODIPY chromophores.

According to the TG experiments, the bulk thermal conversion of BCOD-fused bis-BODIPYs was conducted at 250 °C for 1 h under a reduced pressure and the π-fused bis-BODIPYs **7** and **9** were obtained (Fig. 2). Due to poor solubility in common solvents and instability in solution, spectroscopic identification of **9** could not be done except for UV spectroscopy. When *syn*-**6b** and *anti*-**6b** were treated at a temperature (160 °C) below the inflation point for 1 h *in vacuo*, BCOD-fused π-expanded BODIPYs *syn*-**8** and *anti*-**8** were obtained in good yields.

Structures of the BCOD- and benzene-fused bis-BODIPYs were determined by an X-ray crystallographic analysis. Suitable single crystals of *syn*-**6a**, *anti*-**6a**·PhCl, *syn*-**6b**·$CHCl_3$, *anti*-**6b**·$2CHCl_3$, *syn*-**7**·C_7H_8, and *anti*-**7**·$2C_{10}H_7Cl$ were obtained. All crystals except for *syn*-**6a** contained co-crystallized solvent molecules. The crystal of *anti*-**6a**·PhCl consists of two crystallographically independent bis-BODIPY molecules. In all cases, the BODIPY chromophores are almost flat and the mean deviations of twelve BODIPY atoms from their mean planes lie between 0.021 Å in *anti*-**6b**·$2CHCl_3$ and 0.103 Å in one molecule of *anti*-**6a**·PhCl (Table 1). A maximum deviation of 0.186(2) Å was observed in the boron atom of *syn*-**6a** as observed in crystal structures of the recently prepared mother BODIPY.[20] The dihedral angles between the mean planes of BODIPY chromophores vary from 122.54(3)° in *syn*-**6a** to 134.76(4)° in another molecule of *anti*-**6a**·PhCl. These values are similar to those of bis-porphyrins fused with BCOD.[8b] The observed large widening is ascribed to the crystal packing effect. In fact, the dihedral angles of BCOD skeletons in these bis-BODIPYs are similar to those reported for BCOD-connected dipyrroles **2**,[16] although the dihedral angles of connecting pyrroles are still a little larger. In the case of π-fused bis-BODIPY **7**, the whole chromophores are almost flat (Fig. 3).

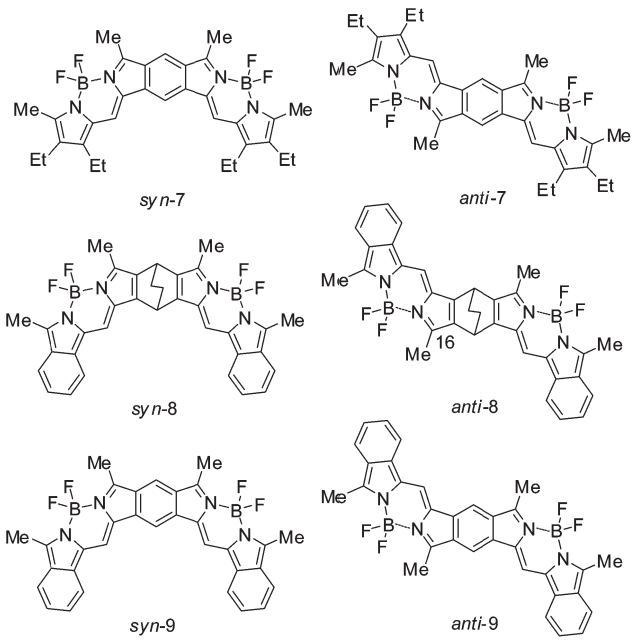

Fig. 2 Structures of π-expanded bis-BODIPYs by thermal treatment.

Electronic spectra of the bis-BODIPYs were next examined. The UV-vis and fluorescence spectra in chloroform are shown in Fig. 4 and 5, and the data are summarized in Table 2 (also see Fig. S1–S9 in ESI†). Quite different spectra were obtained for *syn*- and *anti*-BCOD-connected BODIPYs (*syn*-**6a**,**b** *vs.* *anti*-**6a**, **b**). The *anti*-dimers show strong and sharp absorption bands at 544–545 nm with $\varepsilon = 2.34–2.37 \times 10^5$ M^{-1} cm^{-1} and their fluorescence bands were observed at 550–551 nm with high quantum yields (0.97 for *anti*-**6a** and 0.69 for *anti*-**6b**). Although the absorption bands are slightly red-shifted compared with those of fully alkyl-substituted BODIPYs and the Stokes shift was quite small (6 nm), these molar extinction values are almost twice as large as those of the common BODIPY dyes.[9,21] On the other hand, splitting of the absorption bands is observed in the case of BCOD-fused *syn*-bis-BODIPYs. *syn*-**6a** shows a split absorption band at 503 and 550 nm with $\varepsilon = 7.52 \times 10^4$ and 1.51×10^5 M^{-1} cm^{-1}, respectively. The molar extinction values are similar to those of the common BODIPYs.[9,21] Similarly, *syn*-**6b** shows a band at 504 (5.76×10^4) and 553 (1.09×10^5 M^{-1} cm^{-1}) nm. Fluorescence emission of *syn*-**6a** and *syn*-**6b** is observed at 560 and 561 nm with quantum yields of 0.92 and 0.82, respectively. The difference in the absorption bands between the *syn*- and *anti*-isomers is rationalized by taking the molecular geometry into an account (*vide infra*).

BCOD-connected bis-benzoBODIPYs **8** show a red shift of 24 nm compared to the corresponding *syn*- and *anti*-**6b** (Fig. 5) and this bathochromic shift is less than a half of those observed in the doubly benzo-expanded BODIPYs.[19a,19b,22] A very effective bathochromic shift was achieved by fusion of the BODIPY

Table 1 Deviation from BODIPY mean plane

Compound	BODIPY deviations (Å)				Plane torsion angles		
	Mean				BODIPYs	Pyrroles	BCOD
syn-**6a**	0.060	0.095	C8, 0.126(2)	B2, 0.186(2)	122.54(3)°	129.08(6)°	124.02(9)°
anti-**6a**	0.052	0.054	B1, 0.118(3)	C11, 0.106(2)	134.76(4)°	133.94(8)°	124.2(1)°
	0.103	0.054	B1, 0.183(2)	B2, 0.097(3)	132.66(4)°	130.71(8)°	123.6(1)°
syn-**6b**	0.053	0.067	C2, 0.111(9)	B2, 0.16(2)	132.8(1)°	130.4(3)°	122.7(5)°
anti-**6b**	0.030	0.021	C3, 0.051(3)	C17, 0.042(4)	130.22(5)°	132.1(1)°	123.9(2)°
syn-**7**	0.055		B2, 0.219(5)		4.77(7)°	4.5(1)°	—
anti-**7**	0.026		B, 0.044(6)		0°	0°	—
16/$CHCl_3$	0.024	0.075	B1, 0.045(4)	B2, 0.223(4)	124.71(5)°	123.1(1)°	122.5(2)°
16/PhCl	0.017	0.027	C4, 0.032(2)	C12, 0.050(2)	119.78(3)°	124.00(8)°	122.9(1)°
17	0.036	0.033	C9, 0.085(3)	B2, 0.124(2)	130.73(3)°	129.59(8)°	123.1(1)°

chromophores with benzene and the fusion mode was important. Benzene-fused *syn*-bis-BODIPY *syn*-**7** with C_{2v} symmetry shows the absorption maximum at 692 (2.32×10^5 M^{-1} cm^{-1}) nm, while the absorption maximum of benzene-fused bis-BODIPY *anti*-**7** with C_{2h} symmetry reaches 758 (1.90×10^5 M^{-1} cm^{-1}) nm which is very close to the NIR region. These bis-BODIPYs *syn*-**7** and *anti*-**7** still have strong fluorescence at 703 ($\Phi = 0.72$) and 774 ($\Phi = 0.32$) nm, respectively. Similar Φ values of NIR fluorescence are reported for 8-aza-BODIPY bearing coplanar anisyl-substituents at 3,5-positions,[23] dibenzo-BODIPYs with aryl groups at 3,5-positions,[24] Keio Fluos,[25] and their thia analogs.[26] When the benzoBODIPY chromophores are fused with benzene, both the absorption and fluorescence maxima of C_{2v} and C_{2h} isomers *syn*-**9** and *anti*-**9** are observed in the NIR region: *syn*-**9** absorbs at 775 (1.41×10^5 M^{-1} cm^{-1}) nm and emits at 781 ($\Phi = 0.36$) nm and *anti*-**9** absorbs at 848 (2.04×10^5 M^{-1} cm^{-1}) nm and emits at 868 ($\Phi = 0.04$) nm. These NIR absorptions are 3.7 to 5.2 times larger than the corresponding visible absorptions.

The benzene-fused bis-benzoBODIPYs are labile under aerobic conditions. When *syn*-**9** was dissolved in $CHCl_3$ under aerobic conditions, a strong visible absorption peak at 645 nm with a shoulder (618 nm) appeared at the expense of the 775 nm

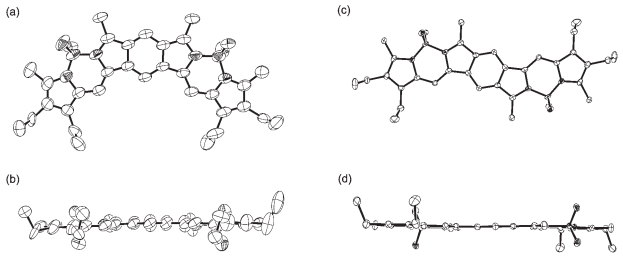

Fig. 3 Ortep drawings (50% probability) of top (a, c) and side (b, d) views of *syn*-**7** and *anti*-**7**. Disordered atoms with smaller occupancy, hydrogen atoms, and co-crystallized solvent molecules are omitted for clarity.

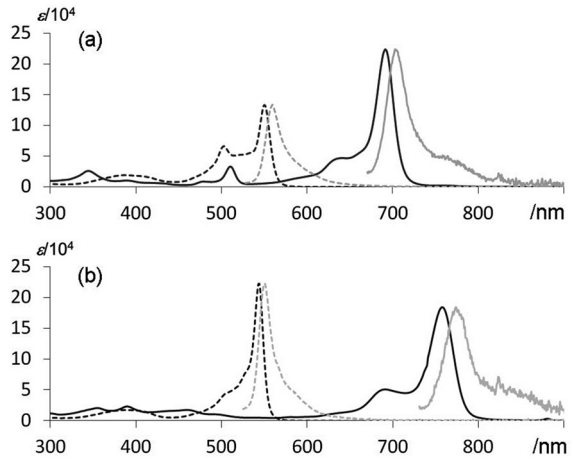

Fig. 4 UV-vis (black) and fluorescence (grey, scaled by arbitrary unit) spectra of *syn*-**6a** (broken lines in **a**), *syn*-**7** (solid lines in **a**), *anti*-**6a** (broken lines in **b**), and *anti*-**7** (solid lines in **b**).

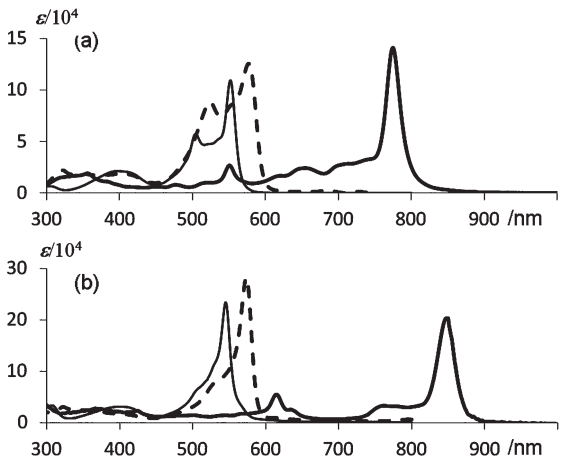

Fig. 5 UV-vis spectra of *syn* derivatives (a), *syn*-**6b**: solid, *syn*-**8**: broken, and *syn*-**9**: bold; and *anti* derivatives (b), *anti*-**6b**: solid, *anti*-**8**: broken, and *anti*-**9**: bold.

Table 2 UV-vis and fluorescence spectra of bis-BODIPYs in $CHCl_3$

Compound	UV-vis (nm) ($\varepsilon/10^4$ M^{-1} cm^{-1})						Fluorescence /nm[a]		Φ
syn-**6a**	387	(2.15)	503	(7.52)	550	(15.10)	560	(10)	0.92
anti-**6a**	388	(1.86)	504	(4.65)	544	(23.70)	550	(6)	0.97
syn-**6b**	397	(2.15)	504	(5.76)	553	(10.90)	561	(8)	0.82
anti-**6b**	403	(3.17)	509	(6.85)	545	(23.40)	551	(6)	0.69
syn-**7**	510	(3.42)	641	(4.86)	692	(23.20)	703	(11)	0.72
anti-**7**	390	(2.40)	691	(5.25)	758	(19.00)	774	(16)	0.32
syn-**8**	400	(1.88)	524	(8.84)	577	(12.60)	591	(14)	0.87
anti-**8**	322	(3.13)	535	(8.33)	569	(28.20)	583	(14)	0.88
syn-**9**	551	(2.70)	655	(2.44)	775	(14.10)	781	(6)	0.36[b]
anti-**9**	615	(5.56)	762	(3.37)	848	(20.40)	868	(20)	0.04
16	403	(2.51)	511	(5.69)	543	(23.50)	549	(6)	0.71[b]
17	328	(2.30)	532	(4.98)	570	(19.20)	580	(10)	0.32[b]
10	613	(0.68)	756	(2.54)	843	(15.80)	861	(18)	0.03[b]

[a] Numerals in the parentheses are Stokes shifts. [b] In CH_2Cl_2.

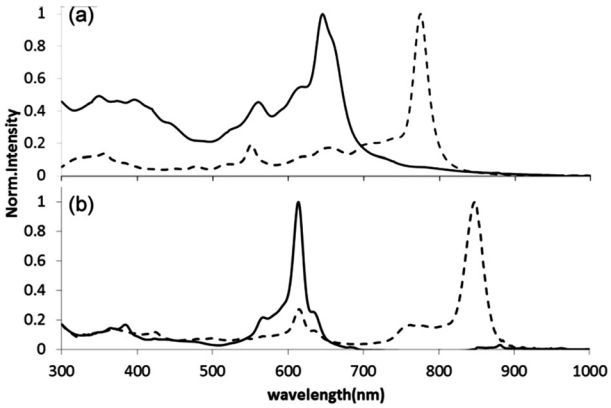

Fig. 6 UV-vis spectra of *syn*-**9** (a) after 0 h (broken) and 20 h (solid); and *anti*-**9** after 0 h (broken) and 6 h (solid).

NIR peak, which completely disappeared after 20 h (Fig. 6). The visible peak of 551 nm in *syn*-**9** also disappeared and a new peak at 562 nm appeared. On the other hand, when *anti*-**9** was dissolved in $CHCl_3$ under air, the visible absorption at 615 nm increased, as the NIR peak of 848 nm decreased. After 6 h, there was no peak over 700 nm. Although we could not identify the decomposition products, the absorption peaks at 645 nm in *syn*-**9** and at 615 nm in *anti*-**9** are imputed to be decomposed compounds formed during the sample preparation for the UV measurements. On the other hand the peak of 551 nm in the visible region of the *syn*-**9** spectrum is thought to be due to *syn*-**9** itself.

In order to get spectroscopic evidence that the final retro-Diels–Alder reaction proceeded smoothly, we planned to prepare the more soluble *anti*-bis-benzoBODIPY **10** (Scheme 2). Ethanoisoindole **1** was reacted with *p*-*tert*-butylbenzoic acid under acidic dehydration conditions to give 3-(*p*-*tert*-butylbenzoyl)-ethanoisoindole **11**, which was then treated with $NaBH_4$ followed by Ac_2O to afford acetoxy derivative **13**.[27] Acidic condensation of *anti*-**2** with **13** provided bis-dipyrromethane tetracarboxylate **14** in good yield. Exhaustive reduction of **14** with $LiAlH_4$ in refluxing THF gave all-methyl derivative **15**, which was oxidatively reacted with $BF_3{\cdot}OEt_2$ to provide bis-BODIPY **16**. Thermogravimetric analysis of **16** revealed three marked weight losses around 100, 170, and 230 °C, which corresponded to evaporation of co-crystallized solvent, extrusion of ethylene from distal ends of BCOD moieties, and extrusion of ethylene from the center BCOD moiety, respectively. In fact, when **16** was heated at 175 and 235 °C *in vacuo* for 1 h, BCOD-connected bis-benzoBODIPY **17** and benzene-connected bis-benzoBODIPY **10** were successfully isolated in 93% and 94% yields, respectively. Benzene-connected bis-benzoBODIPY **10** was unambiguously determined by ^1H NMR analysis. The UV-vis spectral shapes of bis-BODIPYs **10**, **16**, and **17** are almost the same as the corresponding *meso*-unsubstituted derivatives (Fig. 7 and Table 2) except that the visible absorption of **10** at 613 nm is quite weak.

In order to understand the electronic spectra, TD-DFT calculations on bis-BODIPYs (RB3LYP/6-31G(d)) were carried out.[28] The calculated spectra are shown in Fig. 8 and 9. First we discuss the results for BODIPY itself and BCOD-connected

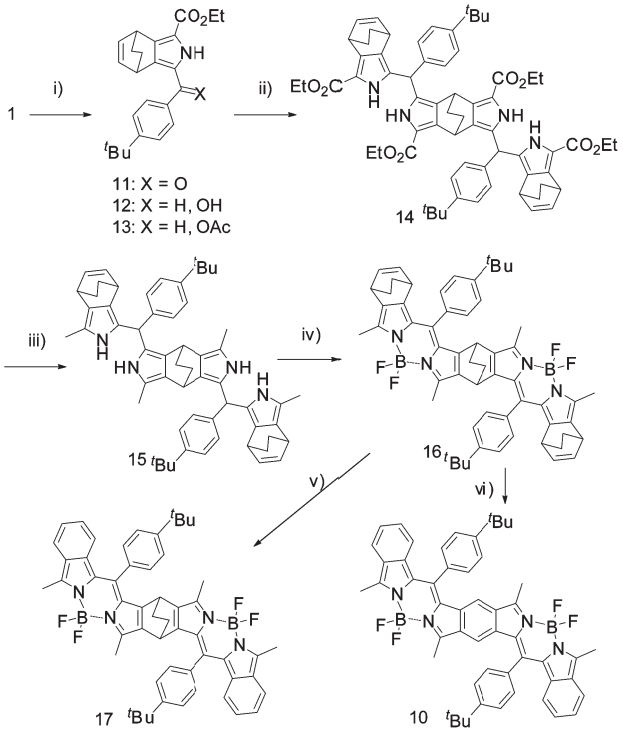

Scheme 2 . (i) 4-*tert*-Butylbenzoic acid, TFAA, TFA, rt; 77%; $NaBH_4$, THF–MeOH, rt; 95%; Ac_2O, DMAP, CH_2Cl_2, rt; 99%. (ii) *anti*-2, pTSA, AcOH, rt; 99%; (iii) $LiAlH_4$, THF, reflux; 86%. (iv) DDQ, CH_2Cl_2, rt; $BF_3{\cdot}OEt_2$, $(i\text{-}Pr)_2EtN$, CH_2Cl_2, rt; 75%. (v) 160 °C, 30 min, 93%. (vi) 235 °C, 30 min, 94%.

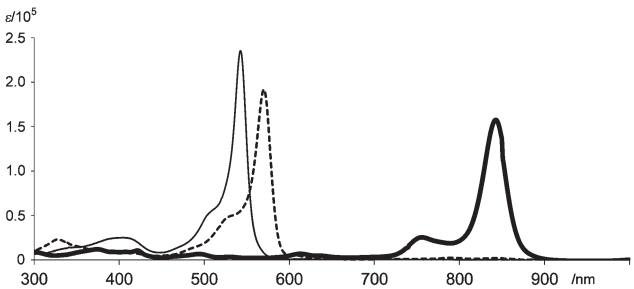

Fig. 7 UV-vis spectra of **16** (solid), **17** (broken), and **10** (bold).

dimers. The TD-DFT results of *anti*-**6a** predict a strong band at 430 nm (oscillator strength, $f = 0.9828$), which corresponds to the observed band at 544 nm. On the other hand, the results of *syn*-**6a** predict three strong bands at 433, 417, and 399 nm, which correspond to the observed bands between 503 and 550 nm. The relevant molecular orbitals of BODIPY and its BCOD-connected dimers are shown in ESI.† The four frontier molecular orbitals of the dimer (HOMO − 1 to LUMO + 1) can be approximately described by symmetric and *anti*-symmetric linear combinations of BODIPY HOMO and LUMO. We denote these orbitals as HOMO(s), HOMO(a), LUMO(s), and LUMO(a). The TD-DFT results revealed that the most prominent peak in the electronic spectra consists of LUMO(a) ← HOMO(s) and LUMO(s) ← HOMO(a) transitions, and that the next prominent peak consists of LUMO(s) ← HOMO − 2. As apparent from the

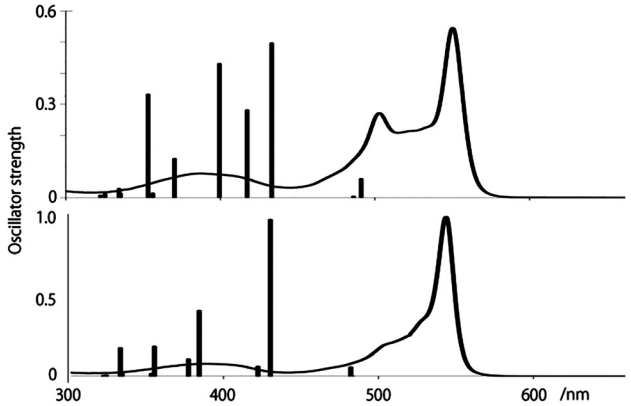

Fig. 8 TD-DFT results of *syn*-**6a** (upper) and *anti*-**6a** (lower) with UV-vis spectra.

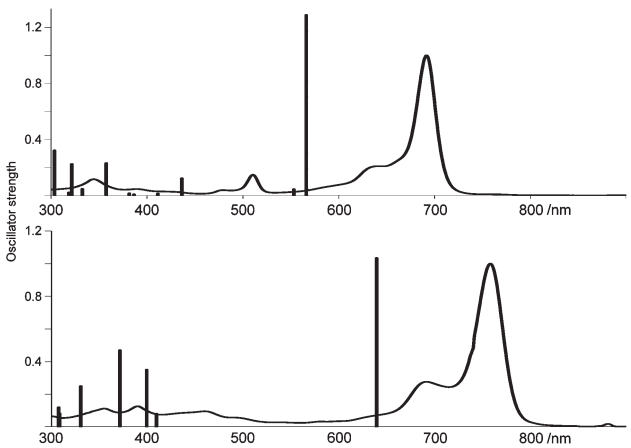

Fig. 9 TD-DFT results of *syn*-**7** (upper) and *anti*-**7** (lower) with UV-vis spectra.

orbital isosurfaces, the LUMO(a, s) ← HOMO(s, a) transitions affect all four pyrrole rings in the molecule, whereas the LUMO(s) ← HOMO − 2 transition only affects the inner two pyrrole rings. Therefore, the former transitions have longer transition dipole moment, and thus longer oscillator strength.

The difference between the *anti* and *syn* isomers is that the terminal pyrrole rings are more distant in the *anti* isomer than in the *syn* isomer. This causes the LUMO(a, s) ← HOMO(s, a) transitions in the *anti* isomer to be even more prominent compared with the LUMO(s) ← HOMO − 2 transition. On the contrary, the LUMO(a, s) ← HOMO(s, a) transitions are less prominent in the *syn* isomer, which results in a clearer observation of the LUMO(s) ← HOMO − 2 transition.

In the cases of benzene-fused bis-BODIPYs **7**, frontier orbitals with nicely separated energy are obtained (Fig. 10). Therefore, the sharp and strong absorptions with the lowest energy mostly consist of simple HOMO–LUMO transitions in both cases: 566 nm (LUMO ← HOMO, 72%, f = 1.2907) in *syn*-**7** and 639 nm (LUMO ← HOMO, 70%, f = 1.0350) in *anti*-**7**. A similar trend in energy diagram is observed in benzene-fused bis-benzoBODIPYs **9**, and the energy gaps are narrower (ESI†). Fig. 10 shows the relevant molecular orbitals of *syn*-**7** and *anti*-**7**, together with their orbital energies. The energies of HOMO

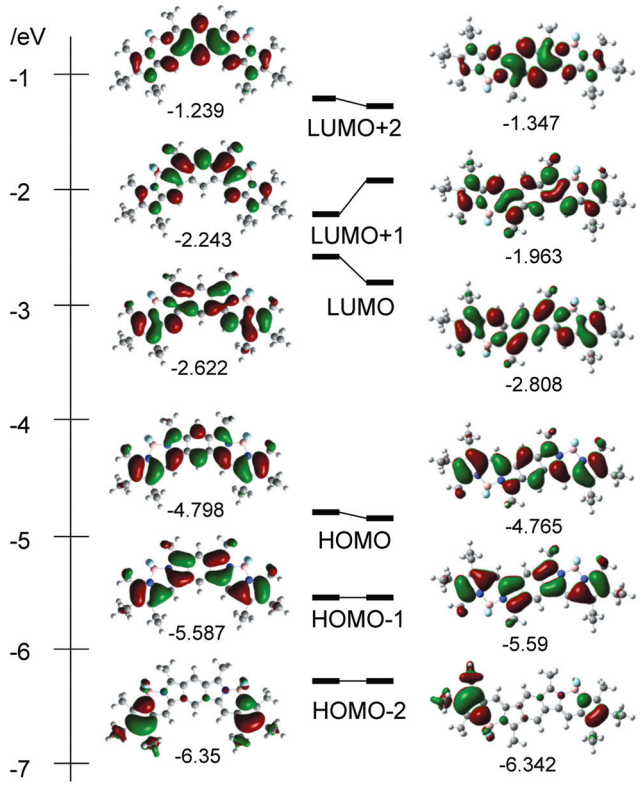

Fig. 10 The calculated frontier orbitals of *syn*-**7** (left) and *anti*-**7** (right).

are similar for *syn*-**7** and *anti*-**7**, whereas the energies of LUMO and LUMO + 1 are markedly different; the LUMO of *anti*-**7** is lower by 0.186 eV than the LUMO of *syn*-**7**, while the LUMO + 1 of *anti*-**7** is higher by 0.28 eV than the LUMO + 1 of *syn*-**7**. The former difference causes the smaller HOMO–LUMO gap in *anti*-**7** than *syn*-**7**, leading to the electronic transition at longer wavelength.

The extra stabilization of LUMO in *anti*-**7** results from the delocalization of the LUMOs of the two BODIPY moieties through the benzo bridge. The AO coefficients on carbons 6 and 13 (see Chart 1) are significant enough to cause delocalization. On the other hand, the LUMO in *syn*-**7** has zero AO coefficients on these carbons, thereby showing no interaction between the LUMOs of the two BODIPY moieties. Actually, these characteristics can be observed not only in the DFT results, but also in the simple Hückel-type calculation of the π-orbitals (ESI†). Therefore, the presence and absence of the interaction between the two BODIPY LUMOs in these isomers are controlled purely by the different topology of the π-electron framework.

Conclusion

We succeeded in the preparation of BODIPY dimers fused at β,β-positions with benzene, namely benzene-fused bis-BODIPYs, which are proved to have sharp and strong absorption and emission bands in the red to NIR region. As the bis-BODIPYs keep good transparency in the other visible region, the dyes are thought to be promising candidates for selective

NIR dyes, although the stability is rather low. Stabilization of bis-BODIPY dyes is the next subject for investigation.

Experimental section

General

Melting points are uncorrected. Unless otherwise specified, NMR spectra were obtained with a JEOL JNM AL-400 spectrometer at ambient temperature by using $CDCl_3$ as a solvent and tetramethylsilane as an internal standard for ^1H and ^{13}C. Mass spectra (EI and FAB) were measured with an MStation spectrometer (JEOL MS-700). MALDI-TOF mass spectra were measured on a Voyger DE Pro (Applied Biosystems) in VBL, Ehime University by using sinapinic acid as matrix. IR spectra were measured with a Horiba FT-720 spectrophotometor. UV-vis and fluorescence spectra were measured on JASCO V-570 and HITACHI F-4500, respectively. Absolute quantum yields were measured on a Hamamatsu Photonics C9920-02. TG analysis was done with an SII Exstar 600 TG/DTA 6200. Elemental analysis was performed on a Yanaco MT-5 elemental analyzer. DMF was distilled under reduced pressure and then stored over MS 4 Å. Pyridine and DMSO were distilled from CaH_2 and stored over MS 4 Å. Other dry solvents were purchased from Kanto Chemical Co. Ethyl isocyanoacetate was kindly provided by The Nippon Synthetic Chemical Industry Co. Ltd. 5-(Acetoxymethyl)pyrrole-2-carboxylates[18,19] and bis-pyrroles **2**[8] were prepared according to the literature.

X-ray crystal structure analysis

Single crystals were prepared by vapor diffusion of isopropanol or methanol into a solution of bis-BODIPYs in $CHCl_3$, chlorobenzene, toluene or 1-chloronaphthalene. The crystals were taken with a Cryoloop and mounted. Determination of cell parameters and collection of reflection intensities were performed by the CrystalClear or RAPID AUTO software.[29] The data were corrected for Lorentz, polarization, and absorption effects. The structures were solved by SIR2004[30] and expanded using the Fourier technique.[31] Hydrogen atoms were placed in calculated positions and refined by using riding models. All calculations were performed by using the CrystalStructure crystallographic software package.[32] Shelxl-97[33] was used for structure refinement. The data were validated by the Platon program.[34] All crystallographic data and the Platon validation results of *syn*-**6a**, *anti*-**6a**·PhCl, *syn*-**6b**·$CHCl_3$, *anti*-**6b**·$2CHCl_3$ *syn*-**7**·PhMe, *anti*-**7**·$2C_{10}H_7Cl$, **16**·$2CHCl_3$, **16**·PhCl, and **17**·PhCl·1/2i-C_3H_7OH are shown in the ESI.†

Materials

General procedure for the condensation of acetoxymethylpyrrole-1-carboxylate 3 and dipyrroledicarboxylate 2. To a stirred solution of **3** (2.0 mmol), and dipyrroledicarboxylate **2** (1.0 mmol) in acetic acid (80 mL) was added *p*-toluenesulfonic acid monohydrate (122 mg, 0.78 mmol) under an inert atmosphere in the dark. After the solution was stirred for 3 h at room temperature, the reaction was quenched with water and the mixture was extracted with chloroform. The organic extract was washed with aqueous saturated $NaHCO_3$, water, and brine, dried over Na_2SO_4, and concentrated *in vacuo*. The residue was chromatographed on silica gel ($CHCl_3$ or 30% EtOAc–hexane).

Diethyl 3,7-bis(5-ethoxycarbonyl-3,4-diethylpyrrol-2-ylmethyl)-4,8-dihydro-4,8-ethanopyrrolo[3,4-*f*]isoindole-1,5-dicarboxylate (*anti*-4a). The reaction of **3a** (0.321 g, 1.18 mmol), and diethyl 4,8-dihydro-4,8-ethanopyrrolo[3,4-*f*]isoindole-1,5-dicarboxylate (*anti*-**2**; 0.165 g, 0.50 mmol) provided 0.273 g (73%) of the title compound as a white powder: mp, 147–149 °C; ^1H NMR: δ 9.10 (br s, 2H), 8.79 (br s, 2H), 4.66 (m, 2H), 4.20–4.30 (m, 8H), 3.92 (m, 4H), 2.71 (m, 4H), 2.42 (m, 4H), 1.71 (m, 4H), 1.31 (t, 6H, J = 7.1 Hz), 1.25 (t, 6H, J = 7.1 Hz), 1.14 (t, 6H, J = 7.6 Hz), 1.04 (t, 6H, J = 7.6 Hz); ^{13}C NMR: δ 161.70, 161.28, 137.22, 133.58, 128.93, 127.87, 124.44, 123.18, 116.92, 113.19, 60.00, 59.70, 31.55, 30.44, 28.32, 23.07, 18.34, 17.01, 16.21, 15.78, 14.36; IR (KBr): 3334, 1701, 1647, 1444, 1263 cm^{-1}; MS (FAB^+): *m*/*z* 743 (M^+ + 1), 742 (M^+), 741 (M^+ − 1); HRMS (FAB^+): $C_{42}H_{54}N_4O_8$ + H^+: 743.4020. Found: 743.4019. Anal. Calcd for $C_{42}H_{54}N_4O_8$ + 1/8C_6H_{14}: C, 68.13; H, 7.46; N, 7.43. Found: C, 67.90, H, 7.33, N, 7.54.

General procedure for reduction of the ester groups. To a stirred solution of bis-dipyrromethane **4** (1.0 mmol) in dry THF (25 mL) was added a 1 M solution of $LiAlH_4$ (6.0 mL, 6.0 mmol) in ether at 0 °C. The mixture was allowed to warm up to room temperature and then the mixture was refluxed for 3 h. After the mixture was cooled to room temperature, the reaction was quenched with water. The resulting suspension was filtered through a Celite pad and the filtrate was extracted with EtOAc. The organic extract was washed with brine, dried over Na_2SO_4, and concentrated *in vacuo*. The residue was passed through a short silica-gel column. This material was used without further purification due to its labile nature under air.

1,5-Dimethyl-3,7-bis(3,4-diethyl-5-methylpyrrol-2-ylmethyl)-4,8-dihydro-4,8-ethanopyrrolo[3,4-*f*]isoindole (*anti*-5a). *anti*-Bis-dipyrromethane tetra ester *anti*-**4a** (0.372 g, 0.50 mmol) was reduced to give 0.239 g (93%) of the title compound as a pale yellow powder: ^1H NMR: δ 7.30 (br s, 2H), 6.84 (br s, 2H), 3.77–3.87 (m, 6H), 2.37–2.45 (m, 8H), 2.10 (s, 6H), 2.08 (s, 6H), 1.65 (m, 4H), 1.11 (t, 6H, J = 7.6 Hz),1.10 (t, 6H, J = 7.6 Hz); ^{13}C NMR: δ 126.69, 125.71, 122.04, 121.01, 120.22, 119.82, 116.58, 115.71, 30.07, 28.80, 22.83, 17.61, 17.53, 16.80, 16.38, 11.10, 11.06; IR (KBr): 3384, 2962, 2931, 2868, cm^{-1}; MS (FAB^+): *m*/*z* 511 (M^+ + 1), 510 (M^+), 509(M^+ − 1); HRMS (FAB^+): $C_{34}H_{46}N_4$ + H^+, 511.3801. Found: 511.3795.

General procedure for the oxidative complexation with BF_3. To a stirred solution of bis-dipyrromethane **5** (0.1 mmol) in dry CH_2Cl_2 (5 mL) was added a suspension of chloranil (50 mg, 0.2 mmol) in CH_2Cl_2 (5 mL) under an inert atmosphere in the dark and the mixture was stirred for 1 h at room temperature. To the mixture were added successively diisopropylethylamine (0.2 mL, 1.2 mmol) and BF_3·OEt_2 (0.16 mL, 1.3 mmol) and the mixture was stirred at room temperature for 2 h. The mixture was quenched with water and then filtered through a Celite pad. The filtrate was washed with aqueous saturated

$NaHCO_3$, water, and brine, dried over Na_2SO_4, and concentrated *in vacuo*. The residue was chromatographed on silica gel.

1,2,8,9-Tetraethyl-4,4,11,11-tetrafluoro-3,5,10,12-tetramethyl-6,13-dihydro-6,13-ethano-4,11-dibora-3a,4a,10a,11a-tetraazabenzo[1,2-*a*:4,5-*a′*]-*s*-indacene (*anti*-6a). *anti*-Bis-dipyrromethane *anti*-**5a** (49 mg, 0.095 mmol) was reacted to give 30.5 mg (53%) of the title compound as pink crystals: ^{1}H NMR: δ 7.03 (s, 2H), 4.38 (m, 2H), 2.60 (q, 4H, J = 7.6 Hz), 2.55 (s, 6H), 2.51 (s, 6H), 2.39 (q, 4H, J = 7.6 Hz), 1.64–1.78 (m, 4H), 1.21 (t, 6H, J = 7.6 Hz), 1.09 (t, 6H, J = 7.6 Hz); ^{13}C NMR: δ 158.18, 148.24, 145.66, 144.64, 134.60, 132.94, 132.20, 126.14, 119.27, 30.93, 28.88, 17.89, 17.30, 16.94, 15.01, 12.96, 12.72; IR (KBr): 2962, 2931, 2871, 1602, 1174 cm^{-1}; UV-vis ($CHCl_3$): λ_{max} (ε/10^4 M^{-1} cm^{-1}), 544 (23.7), 504 (4.65), 388 (1.86) nm; MS (FAB$^+$): m/z 603 (M$^+$ + 1); HRMS (FAB$^+$): $C_{34}H_{40}B_2F_4N_4$ + H$^+$, 603.3453. Found: 603.3459. Anal. Calcd for $C_{34}H_{40}B_2F_4N_4$ + 1/3$CHCl_3$: C, 64.22; H, 6.33; N, 8.73. Found: C, 64.32, H, 6.23, N, 8.44.

General procedure for thermal conversion of bis-BODIPYs with BCOD moieties. A bis-BODIPY compound was weighed in a small test tube and the test tube was placed in a vessel. The vessel was evacuated and placed in a pre-heated glass tube oven at the indicated temperature. After 30 min, the vessel was taken out and cooled to room temperature. The product in the test tube was directly subjected to the analyses.

1,2,10,11-Tetraethyl-4,4,8,8-tetrafluoro-3,5,7,9-tetramethyl-4,8-dibora-3a,4a,7a,8a-tetraazabenzo[1,2-*a*:5,4-*a′*]-*s*-indacene (*syn*-7). *syn*-Bis-BODIPY *syn*-**6** (10.0 mg, 0.017 mmol) was converted at 250 °C to afford 9.2 mg (97%) of the title compound as blue crystals: ^{1}H NMR: δ 8.08 (s + s, 2H), 7.29 (s, 2H), 2.99 (s, 6H), 2.62 (q, 4H, J = 7.6 Hz), 2.51 (s, 6H), 2.42 (q, 4H, J = 7.6 Hz), 1.23 (t, 6H, J = 7.6 Hz), 1.12 (t, 6H, J = 7.6 Hz); ^{13}C NMR: δ 157.34, 149.43, 139.97, 129.77, 129.62, 129.45, 127.76, 118.93, 114.02, 134.76, 108.50, 17.86, 17.24, 17.15, 15.34, 12.98, 12.27; IR (KBr): 1589, 1209, 1186, 1095 cm^{-1}; UV-vis ($CHCl_3$): λ_{max} (ε/10^4 M^{-1} cm^{-1}), 692 (23.2), 641 (4.86), 510 (3.42) nm; MS (FAB$^+$): m/z 574 (M$^+$); HRMS (FAB$^+$): $C_{32}H_{36}B_2F_4N_4$ + H$^+$, 575.3140. Found: 575.3127. Anal. Calcd for $C_{32}H_{36}B_2F_4N_4$ + H_2O: C, 64.89; H, 6.47; N, 9.46. Found: C, 64.56; H, 5.96; N, 9.24.

1,2,8,9-Tetraethyl-4,4,11,11-tetrafluoro-3,5,10,12-tetramethyl-4,11-dibora-3a,4a,10a,11a-tetraazabenzo[1,2-*a*:4,5-*a′*]-*s*-indacene (*anti*-7). The title compound (9.3 mg, 98%) was obtained from *anti*-bis-BODIPY *anti*-**6a** (10 mg 0.017 mmol) at 250 °C as green crystals: ^{1}H NMR: δ 8.15 (s, 2H), 7.27 (s, 2H), 3.03 (s, 6H), 2.65 (q, 4H, J = 7.6 Hz), 2.52 (s, 6H), 2.43 (q, 4H, J = 7.6 Hz), 1.25 (t, 6H, J = 7.6 Hz), 1.12 (t, 6H, J = 7.6 Hz); ^{13}C NMR: δ 155.87, 149.82, 140.27, 132.65, 131.44, 129.85, 129.49, 128.54, 113.57, 113.52, 17.91, 17.27, 17.15, 15.35, 13.06, 12.32; IR (KBr): 1606, 1213, 1184, 1095 cm^{-1}; UV-vis ($CHCl_3$): λ_{max} (ε/10^4 M^{-1} cm^{-1}), 758 (19.0), 691 (5.25), 390 (2.40) nm; MS (FAB$^+$): m/z 575 (M$^+$ + 1), 574 (M$^+$); HRMS (FAB$^+$): $C_{32}H_{36}B_2F_4N_4$ + H$^+$, 575.3140. Found: 575.3146. Anal. Calcd for $C_{32}H_{36}B_2F_4N_4$ + H_2O: C, 64.89; H, 6.47; N, 9.46. Found: C, 64.67; H, 6.34; N, 9.23.

6,6,10,10-Tetrafluoro-5,7,9,11-tetramethyl-8,17-dihydro-8,17-ethano-6,10-dibora-5a,6a,9a,10a-tetraaza-*s*-indaceno[2,3-*b*:6,5-*b′*]difluorene (*syn*-8). *syn*-Bis-BODIPY *syn*-**6b** (5 mg, 0.006 mmol) was heated at 160 °C to give *syn*-**8** quantitatively as a purple powder: mp, 250 °C (decomp.); ^{1}H NMR: δ 7.72–7.80 (m, 4H), 7.52 (m, 2H), 7.31–7.39 (m, 4H), 4.21 (m, 1H), 4.10 (m, 1H), 2.93 (s, 6H), 2.55 (s, 6H), 1.78 (m, 4H); ^{13}C NMR: δ 155.75, 151.96, 146.34, 143.96, 142.05, 137.85, 135.07, 131.76, 130.54, 125.68, 122.77, 119.18, 116.52, 48.79, 46.09, 31.82, 29.62, 13.06, 12.35; IR (KBr): ν_{max} 2946, 1604, 1473, 1226, 1118 cm^{-1}; UV-vis ($CHCl_3$): λ_{max} (ε/10^4 M^{-1} cm^{-1}), 577 (12.6), 524 (8.84), 400 (1.88) nm; MS (FAB$^+$): m/z 591 (M$^+$ + 1), 590 (M$^+$); HRMS (FAB$^+$): Calcd for $C_{34}H_{28}B_2F_4N_4$ + H$^+$, 591.2514. Found: 591.2521.

6,6,15,15-Tetrafluoro-5,7,14,16-tetramethyl-8,17-dihydro-8,17-ethano-6,15-dibora-5a,6a,14a,15a-tetraaza-*s*-indaceno[2,3-*b*:6,7-*b′*]difluorene (*anti*-8). Bis-BODIPY *anti*-**6b** (5 mg, 0.006 mmol) was heated at 160 °C for 30 min and the title compound was obtained in quantitative yield. *anti*-**8**: purple powder; mp, 250 °C (decomp.); ^{1}H NMR: δ 7.72–7.81 (m, 4H), 7.53 (m, 2H), 7.33–7.38 (m, 4H), 4.41 (m, 2H), 2.93 (s, 6H), 2.57 (s, 6H), 1.77 (m, 4H); ^{13}C NMR δ 158.171, 145.68, 141.63, 135.33, 133.40, 131.74, 130.61, 129.27, 125.71, 124.58, 122.72, 119.30, 116.25, 31.94, 30.70, 29.71, 29.50; IR (KBr): ν_{max}, 2938, 1508, 1511, 1227, 1002 cm^{-1}; UV-vis ($CHCl_3$): λ_{max}, (ε/10^4 M^{-1} cm^{-1}), 569 (28.2), 535 (8.33), 322 (3.13) nm; MS (FAB$^+$): m/z 591 (M$^+$ + 1), 590 (M$^+$): HRMS (FAB$^+$): Calcd for $C_{34}H_{38}B_2F_4N_4$ + H$^+$, 591.2514. Found: 591.2521.

6,6,10,10-Tetrafluoro-5,7,9,11-tetramethyl-6,10-dibora-5a,6a,-9a,10a-tetraaza-*s*-indaceno[2,3-*b*:6,5-*b′*]difluorene (*syn*-9). Bis-BODIPY *syn*-**8** (4 mg, 0.007 mmol) was heated at 250 °C for 30 min and the title compound was obtained in quantitative yield. *syn*-**9**: black powder; mp, >350 °C; ^{1}H NMR: δ 7.63–7.73 (m, 4H), 7.52–7.57 (m, 4H), 7.39 (m, 2H), 3.01 (s, 6H), 2.90 (s, 6H); UV-vis ($CHCl_3$): λ_{max} (ε/10^4 M^{-1} cm^{-1}), 775 (14.1), 655 (2.44), 551 (2.70) nm; MS (FAB$^+$): m/z 563 (M$^+$ + 1), HRMS (FAB$^+$): Calcd for $C_{32}H_{24}B_2F_4N_4$ + H$^+$, 563.2201. Found: 563.2200.

6,6,15,15-Tetrafluoro-5,7,14,16-tetramethyl-6,15-dibora-5a,6a,-14a,15a-tetraaza-*s*-indaceno[2,3-*b*:6,7-*b′*]difluorene (*anti*-9). Bis-BODIPY *anti*-**8** (4 mg, 0.007 mmol) was heated at 250 °C for 30 min and the title compound was obtained in quantitative yield. *anti*-**9**: black powder; mp, >350 °C; UV-vis ($CHCl_3$): λ_{max} (ε/10^4 M^{-1} cm^{-1}), 848 (20.4), 762 (3.37), 615 (5.56) nm; MS (FAB$^+$): m/z 562 (M$^+$), HRMS (FAB$^+$): Calcd for $C_{32}H_{24}B_2F_4N_4$ + H$^+$, 563.2201. Found: 563.2217. Anal. Calcd for $C_{32}H_{24}B_2F_4N_4$ + 1/2H_2O: C, 67.29; H, 4.41; N, 9.81. Found: C, 67.59; H, 4.71; N, 9.45. Due to the low solubility, other spectroscopic analyses could not be done.

5,9-Bis(4-*tert*-butylphenyl)-6,6,15,15-tetrafluoro-5,7,14,16-tetramethyl-1,4,8,10,13,17-hexahydro-1,4:8,17:10,13-triethano-6,15-dibora-5a,6a,14a,15a-tetraaza-*s*-indaceno[2,3-*b*:6,7-*b′*]difluorene (16). The title compound was obtained from **15** (0.351 g, 0.429 mmol) in 75% yield (0.293 g) as a diastereomer mixture: red crystals; mp, 157 °C (decomp.); ^{1}H NMR: 7.56 (m, 4H), 7.31 (m, 4H), 6.38 (m, 2H), 6.08 (m, 2H), 3.81 (m, 2H),

2.76 (m, 2H), 2.72 (m, 2H), 2.51 (s, 6H), 2.22 and 2.20 (a pair of singlets, 6H), 1.45 (s, 18H), 1.4–1.1 (m, 12H); ^{13}C NMR (typical signals): δ 152.52, 152.50, 151.18, 151.04, 149.74, 149.66, 148.92, 146.25, 139.52, 138.62, 138.51, 135.71, 135.60, 133.82, 131.61, 128.93, 128.90, 128.61, 128.58, 128.41, 128.11, 127.75, 127.14, 125.30, 125.19, 124.66, 124.63, 124.58, 124.56, 35.26, 35.23, 34.96, 32.96, 32.93, 31.59, 31.54, 31.47, 27.78, 27.70, 27.63, 26.50, 26.44, 25.94, 25.87, 12.71, 12.10, 12.05; UV-vis ($CHCl_3$): λ_{max} ($\varepsilon/10^4$ M^{-1} cm^{-1}), 543 (23.5), 511 (5.69), 403 (2.51) nm; MS (FAB^+): *m/z* 911 ($M^+ + 1$); HRMS (FAB^+): $C_{58}H_{60}B_2F_4N_4 + H^+$, 911.5018. Found: 911.5013. Anal. Calcd for $C_{58}H_{60}B_2F_4N_4 + CHCl_3 + C_3H_7OH$: C, 68.30; H, 6.38; N, 5.14. Found: C, 68.36; H, 6.69; N, 5.28.

5,9-Bis(4-*tert*-butylphenyl)-6,6,15,15-tetrafluoro-5,7,14,16-tetramethyl-8,17-dihydro-8,17-ethano-6,15-dibora-5a,6a,14a,15a-tetraaza-*s*-indaceno[2,3-*b*:6,7-*b′*] difluorene (17). Bis-BODIPY **16** (17.4 mg, 0.019 mmol) was heated at 175 °C for 2 h and 15.1 mg (93%) of the title compound was obtained: black powder; mp, >223 °C; ^{1}H NMR: δ 7.7–7.6 (m, 6H), 7.38 (m, 4H), 7.19 (t, 2H, J = 8.0 Hz), 7.12 (t, 2H, J = 8.0 Hz), 6.39 (d, 2H, J = 8.0 Hz), 2.93 (s, 6H), 2.66 (br s, 2H), 2.23 (s, 6H), 1.6–1.4 (m, 4H), 1.41 (s, 18H); UV-vis ($CHCl_3$): λ_{max} ($\varepsilon/10^4$ M^{-1} cm^{-1}), 570 (19.2), 532 (4.98), 328 (2.30) nm; MS (FAB^+): 855 (M + 1); HRMS (FAB^+): Calcd for $C_{54}H_{52}B_2F_4N_4 + H^+$, 855.4392. Found: 855.4391. Anal. Calcd for $C_{54}H_{52}B_2F_4N_4 + 1/5CHCl_3$: C, 74.10; H, 5.99; N, 6.38. Found: C, 74.05, H, 5.82; N, 6.13.

5,9-Bis(4-*tert*-butylphenyl)-6,6,15,15-tetrafluoro-5,7,14,16-tetramethyl-6,15-dibora-5a,6a,14a,15a-tetraaza-*s*-indaceno[2,3-*b*:6,7-*b′*]difluorene (10). Bis-BODIPY **16** (13.2 mg, 0.014 mmol) was heated at 235 °C for 2 h and 11.3 mg (94%) of the title compound was obtained: black powder; mp, >350 °C; ^{1}H NMR: δ 7.67 (m, 4H), 7.51 (d, 2H, J = 8.0 Hz), 6.98 (t, 2H, J = 8.0 Hz), 6.87 (t, 2H, J = 8.0 Hz), 6.30 (d, 2H, J = 8.0 Hz), 6.22 (s, 2H), 2.83 (s, 6H), 2.53 (s, 6H), 1.53 (s, 18H); UV-vis ($CHCl_3$): λ_{max} ($\varepsilon/10^4$ M^{-1} cm^{-1}), 843 (15.8), 756 (2.54), 613 (0.68) nm; MS (FAB^+): 827 (M + 1); HRMS (FAB^+): Calcd for $C_{52}H_{48}B_2F_4N_4 + H^+$, 827.4079. Found: 827.4064.

Acknowledgements

This work is partially supported by Grant-in-Aids for Scientific Research (23350020, 23655044, and 23108714 (π-space)) from the Japanese Ministry of Education, Culture, Sports, Science and Technology. Some calculations were done at IMS under the cooperative research program (Nanonet).

Notes and references

1 M. Wainwright, *Color. Technol.*, 2010, **126**, 115–126.
2 (*a*) V. J. Pansare, S. Hejazi, W. J. Faenza and R. K. Prud'homme, *Chem. Mater.*, 2012, **24**, 812–827; (*b*) M. Pawlicki, H. A. Collins, R. G. Denning and H. L. Anderson, *Angew. Chem., Int. Ed.*, 2009, **48**, 3244–3266; (*c*) P.-A. Bouit, K. Kamada, P. Feneyrou, G. Berginic, L. Toupet, O. Maury and C. Andraud, *Adv. Mater.*, 2009, **21**, 1151–1154.
3 G. Qian, Z. Zhong, M. Luo, D. Yu, Z. Zhang, Z. Y. Wang and D. Ma, *Adv. Mater.*, 2009, **21**, 111–116.
4 T. H. Lee, J. Y. Ryu, T. H. Kim, S. H. Moon, D. K. Ahn, M. K. Han, E. Y. Cho, I. S. Shon and S. M. Son, *Mol. Cryst. Liq. Cryst.*, 2009, **514**, 289–301.
5 P.-A. Bouit, D. Rauh, S. Neugebauer, J. L. Delgado, E. D. Piazza, S. Rigaut, O. Maury, C. Andraud, V. Dyakonov and N. Martin, *Org. Lett.*, 2009, **11**, 4806–4809.
6 D. Kumaresan, R. P. Thummel, T. Bura, G. Ulrich and R. Ziessel, *Chem.–Eur. J.*, 2009, **15**, 6335–6339.
7 M. Gouterman, *J. Chem. Phys.*, 1959, **30**, 1139–1161.
8 (*a*) S. Ito, K. Nakamoto, H. Uno, T. Murashima and N. Ono, *Chem. Commun.*, 2001, 2696–2697; (*b*) H. Uno, K. Nakamoto, K. Kuroki, A. Fujimoto and N. Ono, *Chem.–Eur. J.*, 2007, **13**, 5773–5784.
9 A. Loudet and K. Burgess, *Chem. Rev.*, 2007, **107**, 4891–4932.
10 V. J. Pansare, S. Hejazi, W. J. Faenza and R. K. Prud'homme, *Chem. Mater.*, 2012, **24**, 812–827.
11 (*a*) C. Jiao, K.-W. Huang and J. Wu, *Org. Lett.*, 2011, **13**, 632–635; (*b*) C. Jiao, L. Zhu and J. Wu, *Chem.–Eur. J.*, 2011, **17**, 6610–6614.
12 A. Iqbal, M. Jost, R. Kirchmayr, J. Pfenninger, A. Rochat and O. Wallquist, *Bull. Soc. Chim. Belg.*, 1988, **97**, 615–643.
13 (*a*) G. M. Fischer, E. Daltrozzo and A. Zumbusch, *Angew. Chem., Int. Ed.*, 2011, **50**, 1406–1409; (*b*) G. M. Fischer, M. Isomäki-Krondahl, I. Göttker-Schnetmann, E. Daltrozzo and A. Zumbusch, *Chem.–Eur. J.*, 2009, **15**, 4857–4864; (*c*) G. M. Fischer, A. Ehlers, A. Zumbusch and E. Daltrozzo, *Angew. Chem., Int. Ed.*, 2007, **46**, 3750–3753.
14 (*a*) T. Itoh, T. Murashima, H. Uno and N. Ono, *Chem. Commun.*, 1998, 1661–1662; (*b*) S. Ito, N. Ochi, T. Murashima, H. Uno and N. Ono, *Heterocycles*, 2000, **52**, 399–411.
15 K. D. Johnstone, W. A. Pearce and S. M. Pyke, *J. Porphyrins Phthalocyanines*, 2002, **6**, 661–672.
16 H. Uno, S. Ito, M. Wada, H. Watanabe, M. Nagai, A. Hayashi, T. Murashima and N. Ono, *J. Chem. Soc., Perkin Trans. 1*, 2000, 4347–4355.
17 (*a*) H. Uno, M. Tanaka, T. Inoue and N. Ono, *Synthesis*, 1999, 471–474; (*b*) M. Wada, S. Itoh, H. Uno, T. Murashima, N. Ono, T. Urano and Y. Urano, *Tetrahedron Lett.*, 2001, **42**, 6711–6713.
18 Y. Murakami, S. Yamada, Y. Matsuda and K. Sakata, *Bull. Chem. Soc. Jpn.*, 1978, **51**, 123–129.
19 (*a*) T. Okujima, N. Komobuchi, Y. Shimizu, H. Uno and N. Ono, *Tetrahedron Lett.*, 2004, **45**, 5461–5464; (*b*) S. Ito, N. Ochi, T. Murashima, H. Uno and N. Ono, *Heterocycles*, 2000, **52**, 399–411; (*c*) H. Uoyamaa, T. Takiuea, K. Tominagaa, N. Ono and H. Uno, *J. Porphyrins Phthalocyanines*, 2009, **13**, 122–135.
20 A. Schmitt, B. Hinkeldey, M. Wild and G. Jung, *J. Fluoresc.*, 2009, **19**, 755–758; K. Tram, H. Yan, H. A. Jenkins, S. Vassiliev and D. Bruce, *Dyes Pigm.*, 2009, **82**, 392–395; I. J. Arroyo, R. Hu, G. Merino, B. Z. Tang and E. Peña-Cabrera, *J. Org. Chem.*, 2009, **74**, 5719–5722.
21 (*a*) G. Ulrich, R. Ziessel and A. Harriman, *Angew. Chem., Int. Ed.*, 2008, **47**, 1184–1201; (*b*) R. Ziessel, G. Ulrich and A. Harriman, *New J. Chem.*, 2007, **31**, 496–501.
22 Z. Shen, H. Röhr, K. Rurack, H. Uno, M. Spieles, B. Schulz, G. Reck and N. Ono, *Chem.–Eur. J.*, 2004, **10**, 4853–4871; T. Okujima, Y. Tomimori, J. Nakamura, H. Yamada, H. Uno and N. Ono, *Tetrahedron*, 2010, **66**, 6895–6900.
23 W. Zao and E. Carreira, *Angew. Chem., Int. Ed.*, 2005, **44**, 1677–1679.
24 Y. Kubo, Y. Minowa, T. Shoda and K. Takeshita, *Tetrahedron Lett.*, 2010, **51**, 1600–1602.
25 K. Umezawa, Y. Nakamura, H. Makino, D. Citterio and K. Suzuki, *J. Am. Chem. Soc.*, 2008, **130**, 1550–1551.
26 S. G. Awuah, J. Polreis, V. Biradar and Y. You, *Org. Lett.*, 2011, **13**, 3884–3887.
27 B. Jolicoeur, E. E. Chapman, A. Thompson and W. D. Lubell, *Tetrahedron*, 2006, **62**, 11531–11563.
28 M. J. Frisch, G. W. Trucks, H. B. Schlegel, G. E. Scuseria, M. A. Robb, J. R. Cheeseman, J. A. Montgomery, Jr., T. Vreven, K. N. Kudin, J. C. Burant, J. M. Millam, S. S. Iyengar, J. Tomasi, V. Barone, B. Mennucci, M. Cossi, G. Scalmani, N. Rega, G. A. Petersson, H. Nakatsuji, M. Hada, M. Ehara, K. Toyota, R. Fukuda, J. Hasegawa, M. Ishida, T. Nakajima, Y. Honda, O. Kitao, H. Nakai, M. Klene, X. Li, J. E. Knox, H. P. Hratchian, J. B. Cross, V. Bakken, C. Adamo, J. Jaramillo, R. Gomperts, R. E. Stratmann, O. Yazyev, A. J. Austin, R. Cammi, C. Pomelli, J. W. Ochterski, P. Y. Ayala, K. Morokuma, G. A. Voth, P. Salvador, J. J. Dannenberg, V. G. Zakrzewski, S. Dapprich, A. D. Daniels, M. C. Strain, O. Farkas, D. K. Malick, A. D. Rabuck, K. Raghavachari, J. B. Foresman, J. V. Ortiz, Q. Cui, A. G. Baboul, S. Clifford, J. Cioslowski, B. B. Stefanov, G. Liu, A. Liashenko,

P. Piskorz, I. Komaromi, R. L. Martin, D. J. Fox, T. Keith, M. A. Al-Laham, C. Y. Peng, A. Nanayakkara, M. Challacombe, P. M. W. Gill, B. Johnson, W. Chen, M. W. Wong, C. Gonzalez and J. A. Pople, *GAUSSIAN 03 (Revision E.01)*, Gaussian, Inc., Wallingford CT, 2004.

29 *CrystalClear and RAPID AUTO: Reflection Collection and Data Reduction Packages*, Rigaku, 3-9-12 Akishima, Tokyo, Japan, and Rigaku/MSC (9009 New Trails Dr., The Woodlands, TX 77381 USA).

30 *SIR2004: An Improved Tool for Crystal Structure Determination and Refinement*, Istituto di Gristallografia, Italy; M. C. Burla, R. Caliandro, M. Camalli, B. Carrozzini, G. L. Cascarano, L. De Caro, C. Giacovazzo, G. Polidori and R. Spagna, *J. Appl. Crystallogr.*, 2005, **38**, 381–388.

31 P. T. Beurskens, G. Beurskens, R. de Gelder, S. Garcia-Granda, S. O. Gould and J. M. M. Smits, *The Dirdif-2008 Program System*, Crystallography Laboratory, University of Nijmegen, The Netherlands, 2008.

32 *CrystalStructure Ver. 4.0.1, Crystal Structure Analysis Package*, Rigaku, 3-9-12 Akishima, Tokyo, Japan, and Rigaku/MSC (9009 New Trails Dr., The Woodlands, TX 77381 USA).

33 *Shelxl-97: Program for the Refinement of Crystal Structures from Diffraction Data*, University of Göttingen, Göttingen, Germany; "A short history of SHELX"; G. M. Sheldrick, *Acta Crystallogr., Sect. A: Found. Crystallogr.*, 2008, **A64**, 112–122.

34 Platon: A. L. Spek, *A Multipurpose Crystallographic Tool*, Utrecht University, Utrecht, The Netherland, 2003; A. L. Spek, *J. Appl. Crystallogr.*, 2003, **36**, 7–13.